Anterior Segment OCTA of Melanocytic Lesions of the Conjunctiva and Iris

NIELS J. BROUWER, MARINA MARINKOVIC, JACO C. BLEEKER, GREGORIUS P.M. LUYTEN, AND MARTINE J. JAGER

• PURPOSE: To study the feasibility and diagnostic value of vascular imaging using optical coherence tomography (OCT)-angiography (OCTA) of melanocytic lesions of the conjunctiva and iris.
• DESIGN: Cross-sectional study.
• METHODS: Twenty-five patients with an untreated conjunctival lesion (5 melanoma, 13 nevus, 7 primary acquired melanosis [PAM]) and 52 patients with an untreated iris lesion (10 melanoma, 42 nevus) were included. Patients were imaged using a commercially available OCTA device, with the addition of an anterior segment lens and manual focussing. Tumor vessel presence, vascular patterns and vascular density were assessed.
• RESULTS: Good OCTA images were obtained in 18 of 25 conjunctival lesions and 42 of 52 iris lesions. Failure was caused by lack of patient cooperation, an unfavorable location, or mydriasis. In all imaged conjunctival lesions and 77% of iris lesions, vascular structures were detected. Conjunctival melanoma and nevi demonstrated the same intralesional tortuous patterns, whereas vasculature in eyes with PAM was similar to normal conjunctiva. Both iris melanoma and nevi demonstrated tortuous patterns, distinct from the radially oriented normal iris vasculature.
• CONCLUSIONS: Optical coherence tomography angiography (OCTA) allows for noninvasive imaging of the vasculature in melanocytic lesions of the conjunctiva and iris. Good image quality depends highly on patient cooperation and lesion characteristics. Differentiation of benign and malignant lesions was not possible. New software is called for to improve image acquisition and analysis. (Am J Ophthalmol 2021;222:137–147. © 2020 The Authors. Published by Elsevier Inc. This is an open access article under the CC BY license (http://creativecommons.org/licenses/by/4.0/).)

NEVI OF THE CONJUNCTIVA OR IRIS ARE RELATIVELY common conditions, requiring no further treatment apart from close observation or excision for cosmetic reasons.[1,2] Malignant melanoma of the conjunctiva or iris, however, have the potential to metastasize, and treatment is generally indicated.[3,4] Clinical differentiation of these entities can be challenging,[1,2] despite imaging techniques such as ultrasonography and OCT of the anterior segment.

A factor that can differentiate melanocytic lesions of the eye is tumor vascularity. Fluorescein angiography (FA) has long been used to differentiate between benign and malignant choroidal lesions.[5,6] Since the early 1970s, FA was used to study iris lesions as well.[7,8] Benign iris lesions demonstrated less chaotic patterns than malignant lesions and even showed silencing (masking) of the FA signal,[9–12] but there has been no full agreement on all FA findings, such as orderly patterns or leakage of dye.[11,13–15] The usefulness of dye-based angiography of the conjunctiva has long been limited because low-molecular-weight fluorescein easily leaks from vessels,[16] and to these authors' knowledge, no studies of dye-based angiography of the intrinsic vasculature of conjunctival melanoma, nevi or primary acquired melanosis (PAM) exist. As a drawback for FA, the technique is relatively time consuming and requires injection of dye, with potential adverse events.[17,18]

A new and noninvasive technique to study ocular vasculature is OCT-angiography (OCTA). This technique has been developed to depict the retinal vasculature.[19] By measuring changes in sequential cross-sectional images (B-scans), flow can be visualized without the need for intravenous dye injection. OCTA has several additional advantages, such as high image quality, visualization of vessels at different depths, and easy operating instructions. Recently it was demonstrated that, apart from imaging retinal vessels, OCTA can image tumor vessels in choroidal melanoma and nevi as well.[20–22]

With some adjustments to the conventional posterior segment technique (using an anterior segment lens, and (manual) focussing on the ocular surface), OCTA can detect vascular flow in the anterior segment as well.[23] Small series have demonstrated proof of principle in iridal, corneal, and conjunctival tissue.[24–26] Most commercially available OCTA devices do not support the full range of image acquisition and analysis modes for the anterior segment that were developed for retinal images; however and obtaining good image quality can therefore be challenging.[27] Using OCTA of the anterior segment, Skalet and associates[28] demonstrated vascular patterns in pigmented lesions of the iris and found differences in

AJO.com Supplemental Material available at AJO.com.
Accepted for publication Sep 3, 2020.
From the Department of Ophthalmology, Leiden University Medical Center, Leiden, The Netherlands.
Inquiries to Marina Marinkovic, Department of Ophthalmology, Leiden University Medical Center, PO Box 9600, 2300 RC Leiden, the Netherlands; e-mail: m.marinkovic@lumc.nl

TABLE 1. Characteristics of the Included Patients

	Conjunctival Melanoma	Conjunctival Nevus	PAM	Iris Melanoma	Iris Nevus
	n = 5	n = 13	n = 7	n = 10	n = 42
	Cases (%)	Cases (%)	Cases (%)	Cases (%)	Cases (%)
Sex					
Male	2 (40)	4 (31)	2 (29)	5 (50)	23 (55)
Female	3 (60)	9 (69)	5 (71)	5 (50)	19 (45)
Mean age, y	61.0	38.2	57.7	60.4	61.6
Mean thickness, mm[a]	0.77	NA	NA	2.0	1.1
Mean LBD, mm	6.6	3.3	NA	6.4	3.9
Lesion pigmentation					
Amelanotic/light	3 (60)	5 (38)	3 (43)	2 (20)	15 (36)
Medium	1 (20)	4 (31)	4 (57)	5 (50)	13 (31)
Dark	1 (20)	4 (31)	0 (0)	3 (30)	14 (33)
Location in the conjunctiva					
Bulbar	5 (100)	7 (54)	7 (100)	NA	NA
Plica/caruncle	0 (0)	6 (46)	0 (0)	NA	NA
Location in an iris quadrant					
Superior	NA	NA	NA	1 (10)	6 (14)
Inferior	NA	NA	NA	6 (60)	20 (48)
Temporal/nasal	NA	NA	NA	3 (30)	16 (38)
Mean clock h, size	NA	NA	NA	2.4	1.7
Secondary cataract	NA	NA	NA	0 (0)	1 (2)
IOP >20 or IOP treatment, mm Hg	NA	NA	NA	3 (30)	7 (17)
Ectropion uveae	NA	NA	NA	6 (60)	20 (48)
Iris color					
Blue	NA	NA	NA	10 (100)	37 (88)
Green	NA	NA	NA	0 (0)	4 (10)
Brown	NA	NA	NA	0 (0)	1 (2)

IOP = intraocular pressure; LBD = largest basal diameter; NA = not applicable; PAM = primary acquired melanosis.
Values are n (%).
[a]Data for lesion thickness (assessed by histology) were available for all conjunctival melanoma but none of the conjunctival nevi or PAM.

vascular density between 3 iris nevi and 3 iris melanomas.[28] To the present authors' knowledge, no studies of OCTA of melanocytic lesions of the conjunctiva exist.

The feasibility of OCTA of melanocytic lesions of the conjunctiva and iris were studied, with a second aim of identifying differentiating features between benign and malignant lesions.

METHODS

• **PATIENT SELECTION:** Patients were recruited at the Leiden University Medical Center (LUMC), a tertiary hospital for ocular oncology in The Netherlands. Included were patients with a treatment-naïve conjunctival melanoma (n = 5), conjunctival nevus (n = 13), primary acquired melanosis (PAM, n = 7), iris melanoma (n = 10), or iris nevus (n = 42). Patients were seen and conditions were diagnosed in the ophthalmo-oncology clinic of the Department of Ophthalmology. Standard clinical examinations were performed including slit lamp examination and anterior segment photography.

Approval for this cross-sectional study was obtained from the Institutional Ethics Review Board of the LUMC (approval number P17.134). The tenets of the declaration of Helsinki were followed. All patients signed an informed consent.

• **CONJUNCTIVAL LESIONS:** All 5 conjunctival melanoma cases were confirmed by histology. In 9 of 13 cases, the diagnosis of conjunctival nevus was confirmed by histology; 4 cases were diagnosed clinically (with circumscribed lesions and cysts; in 3 of those cases, the lesion had not changed in more than 30 years (and in 1 case in more than 9 years).[2,29] Six cases were diagnosed with PAM, which was confirmed by biopsy (showing 4 cases with atypia and 2 without), whereas 1 case was diagnosed clinically (with a unilateral diffuse lesion and variable presence [ie, "waxing and waning"]).[2] Where possible, the thickness of conjunctival lesions was determined by

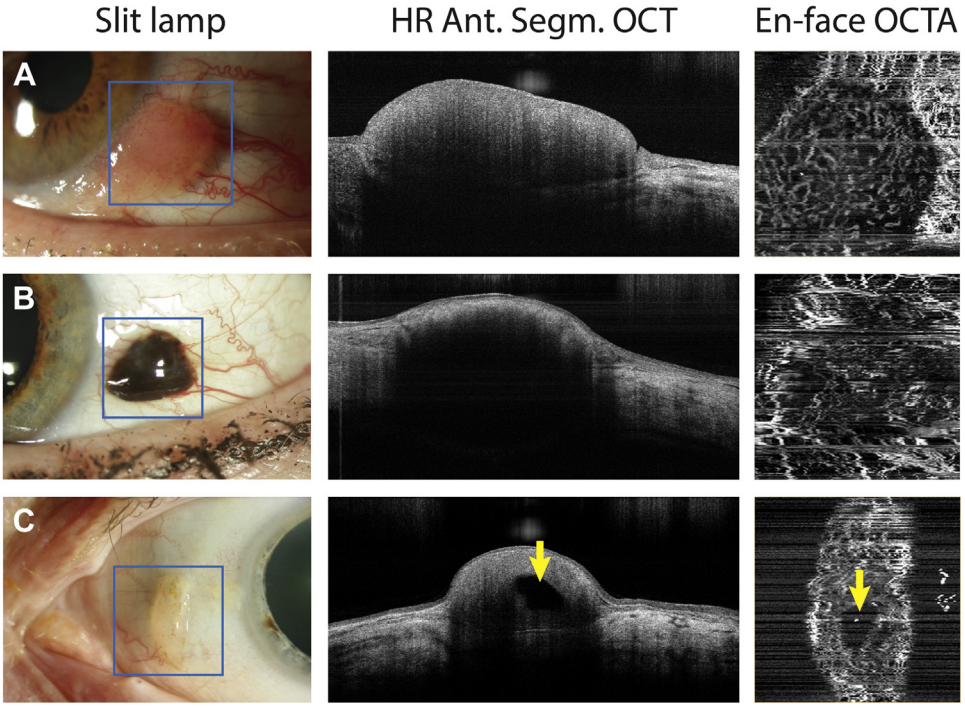

FIGURE 1. Conjunctival melanoma and nevi. Vascular structures were seen in all conjunctival lesions. Image quality was higher in lightly pigmented lesions (Patient A, conjunctival melanoma) compared to those with dark lesions (Patient B, conjunctival melanoma), and had better signal penetrance. In conjunctival nevi (Patient C), cysts were often seen as areas with no apparent vasculature. All optical coherence tomography angiography scans were acquired in a 3 × 3-mm setting.

histology, the largest basal diameter was assessed by clinical measurements.

• **IRIS LESIONS:** Ultrasonography was performed on all iris lesions to determine lesion size and extent. Iris lesions were diagnosed by clinical and ultrasonographic characteristics. Diagnosis of melanoma was based on tumor size, evidence of growth, ultrasonographic structure, visibility of vessels, and secondary symptoms such as elevated intraocular pressure or cataract.[30–33] Biopsy analyses were only performed in 2 patients, confirming the clinical diagnosis of 1 iris nevus and 1 iris melanoma.

• **OCTA ACQUISITION AND ANALYSIS:** Images were taken prior to any surgical procedure. OCTA scans were performed using an 'RS 3000 Advance' OCTA device (Nidek, Ltd, Gamagori, JA). A device-specific anterior segment lens was inserted. Patients were positioned in front of the device and instructed to focus on either the external fixator light or gaze in a specific direction. Conjunctival lesions were assessed under dimmed light conditions, and iris lesions were assessed under ambient room lighting to create miosis. First, the anterior segment lens was positioned close to the ocular surface to retrieve a signal from the tissue of interest. Second, the focus was manually adjusted to obtain the clearest view. Images were acquired in retinal mode (while focussing on the conjunctiva or iris), with an image size setting of 3 × 3-mm for all patients (for detailed vessel density calculation), and additional scans of up to 9 × 9-mm were taken for larger lesions (for an overview). Image resolution of all scans (regardless of the size of the depicted area) was 256 × 256 pixels. Images were acquired in "skip mode," as the trace function (developed for retinal imaging) proved not suitable to trace the surface of the conjunctiva or iris.

Images were assessed using the device-specific software Navis-Ex version 1.8 software (Nidek). As the automated image segmentation (developed to delineate retinal layers) misinterpreted the conjunctival and iridal structures, 2 segmentation lines were drawn manually to include the lesion of interest.

First, it was recorded if an acceptable image was obtained, that is, if a full scan was completed, including the lesion of interest, without major surface-trace issues resulting in total artifacts. Second, the presence of vessel-like segments was noted, in healthy conjunctiva or iris tissue (to assess successful imaging) and at the site of the lesion. When vessels were visible in the lesion, image quality of those vessels was graded subjectively as (grade 1) clear visibility, (grade 2) medium visibility, or (grade 3) nonclear visibility.

Vessel density (VD) was quantified in the en-face images of a subset of patients using ImageJ software (National Institutes of Health, Bethesda, Maryland, USA). The lesion of interest was selected manually, and binarization was

TABLE 2. Comparison between the Visibility of Vessels (Image Quality) and Lesion Characteristics

Image Quality	Clear n = 13 Cases (%)	Medium n = 18 Cases (%)	Nonclear n = 21 Cases (%)	*P* Value
Lesion pigmentation (all)				
Amelanotic/light	9 (69)	7 (39)	5 (24)	.006 [a]
Medium	3 (23)	9 (50)	9 (43)	
Dark	1 (8)	2 (11)	7 (33)	
Mean patient age	44.2	60.5	61.2	.019 [b c]
Location (Conjunctival. lesions)	n = 4	n = 10	n = 4	
Bulbar	4 (100)	9 (90)	2 (50)	.065 [a]
Plica/caruncle	0 (0)	1 (10)	2 (50)	
Location (iris lesions)	n = 9	n = 8	n = 17	
Superior	0 (0)	0 (0)	2 (12)	.45 [a]
Inferior	5 (56)	7 (88)	9 (53)	
Temporal/Nasal	4 (44)	1 (12)	6 (35)	

Values are n (%).
[a]Linear-by-linear test;
[b]Kruskal-Wallis test;
[c]*P* value comparing age in groups "clear" vs "medium" quality is $P = .022$ (Mann-Whitney *U* test).

performed with an Otsu threshold.[34] In the area of interest, pixels attributed to vessels (those above the threshold) were counted and expressed as a percentage of the total selected area size.

In conjunctival lesions, VD was first calculated in all bulbar lesions (excluding lesions of the caruncle or plica), and a second analysis was performed excluding heavily pigmented and grade 3 quality lesions (to limit the influence of signal masking by heavy pigmentation and noise). In iris lesions, the VD was similarly calculated in those cases with a light or modest tumor pigmentation and grades 1-2 image quality. The en-face area of ectropion uveae was excluded from analysis.

• **ANTERIOR SEGMENT-OCT IMAGING:** Each lesion was assessed with high-resolution anterior segment (AS)-OCT using the same imaging device that was applied for AS-OCTA. The anterior segment lens was inserted, capturing images in regular anterior segment mode. Images with a width of 6.0 mm were acquired in a radial pattern at "ultra fine" resolution.

• **STATISTICAL ANALYSIS:** Statistical analyses were performed using SPSS version 23 software (IBM, Armonk, New York, USA). For all analyses, *P* values $< .05$ were considered significant. Differences between continuous data were tested using the Mann-Whitney *U* or Kruskal-Wallis test. Differences between discrete data were tested with the Fisher exact or linear-by-linear test.

• **FOV WHEN EXAMINING THE ANTERIOR SEGMENT:** Due to different optics when examining the anterior segment, the automated scales to measure retinal or choroidal structures were not fully applicable to this study. To determine the field of view (FOV) of the anterior segment, a calliper was placed with a fixed width of 9.0 mm in front of the anterior segment lens and a scan was acquired with a setting of 9 × 9-mm (Supplemental Figure; available at AJO.com). By comparing the ratio between the calliper size and the scanned image size, the true FOV in the settings proved to be 12.3 × 12.3-mm. A similar technique to determine the FOV of anterior segment OCTA was reported by Liu and associates,[35] resulting in comparable (yet device-specific) values.

RESULTS

• **PATIENTS:** Twenty-five patients with conjunctival lesions were included. Five of the lesions (20%) were diagnosed as conjunctival melanoma, 13 (52%) as conjunctival nevus, and 7 (28%) as PAM. The mean age of patients with a conjunctival lesion was 48.2 years. All lesions were epibulbar or involved the plica or caruncle; all 5 conjunctival melanoma were stage pT1a (TNM staging system, 8th edition).[36]

Fifty-two patients with an iris lesion were included. Ten of them (19%) received diagnoses of iris melanoma and 42 (81%) of iris nevus. The mean age of patients with an iris

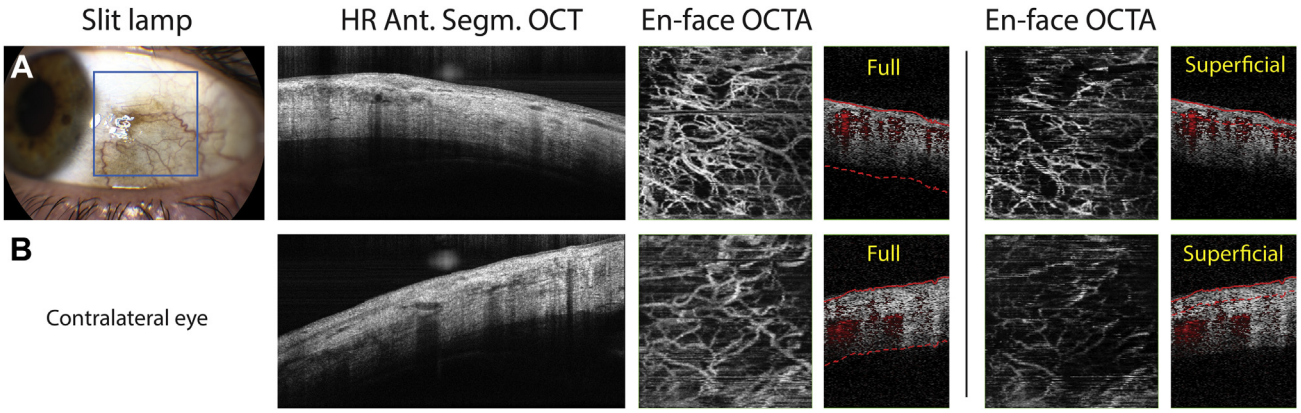

FIGURE 2. PAM and healthy conjunctiva. The vascular pattern in eyes with PAM (A, top row) was similar to the pattern in the contralateral eye with unaffected conjunctiva (B, bottom row), although the meshwork might have been somewhat finer. Both a full-thickness selection of tissue (including sclera and conjunctiva) and a superficial layer selection (approximating the conjunctival epithelium) are presented. All OCTA scans were acquired in a 3 × 3-mm setting. PAM = primary acquired melanosis

lesion was 61.4 years. The Tumor-Node-Metastasis (TNM) stage of the iris melanoma was stage T1a (n = 6), T1b (n = 1), T1c (n = 1), T2a (n = 1); 1 case of predominantly ciliary body melanoma with significant iris involvement was stage T2b.[37] Further patient and tumor characteristics are provided in Table 1.

• **CONJUNCTIVAL LESIONS:** OCTA scans were acquired successfully in 4 of 5 (80%) conjunctival melanoma patients, and 8 of 13 (62%) conjunctival nevus patients. Causes for failure were patient noncooperation (n = 3), lack of focus (n = 2 caruncular lesions), or a bulbar location behind the upper eyelid (n = 1). Manual lifting of the upper eye lid proved not feasible as this resulted in minor movements that hampered the investigation (Supplemental Table; available at AJO.com).

In all 4 successfully imaged conjunctival melanoma and all 8 successfully imaged conjunctival nevi, tortuous vascular structures were detected, distinct from the adjacent conjunctiva (Figure 1). Image quality was better in lightly pigmented lesions compared to dark lesions (Table 2). The plica/caruncle proved difficult to image due to its irregular shape (Table 2). In many nevi, cysts were observed that lacked vascularity. No clear differences were seen between vascular patterns of conjunctival nevi and melanoma.

In 6 of 7 patients (86%) with PAM, OCTA scans were acquired successfully. In 1 case, the lesion proved small and was misidentified during scanning. Vascular structures were detected in all images, both when the full conjunctiva and sclera were selected and when only a superficial layer of tissue (approximating the epithelium) was selected for analysis (Figure 2). The vasculature at the area of PAM appeared similar to the normal conjunctival vessels of the contralateral eye, although in PAM the vasculature appeared to be somewhat finer (Figure 2).

The median VD of quantified bulbar lesions was 35.5% in conjunctival melanoma (n = 4), and 32.5% in conjunctival nevi (n = 5) ($P = .62$). In a further selection of light and medium pigmented cases only, this was 38.3% (melanoma, n = 3) and 37.0% (nevi, n = 3) ($P = .51$) (Table 3). The median VD of PAM was 40.3% (n = 5), whereas that of paired conjunctiva tissue of contralateral eyes was 41.1% ($P = .14$). The VD was decreased in heavily pigmented conjunctival lesions compared to lightly pigmented lesions (median VD, 29.1%, n = 3; and 38.4%, n = 12; $P = .014$) (Figure 3). The presence of cysts was noticed: cysts were seen on scans in 0 of 6 melanoma, 4 of 8 nevi, and 0 of 6 PAM, $P = .046$.

• **IRIS LESIONS:** OCTA scans were acquired successfully in 9 of 10 patients (90%) with iris melanoma and 35 of 42 patients (83%) with iris nevi. Unsuccessful acquisition was due to patient noncooperation (n = 4), pharmacological mydriasis (n = 2), a lesion located too far in the ciliary body (n = 1), or a location behind the upper eyelid (n = 1). Similar to the investigation of conjunctival lesions, manual lifting of the eyelid proved not to be feasible as this induced movement (Supplemental Table; available at AJO.com).

Vascular structures were seen in the area of the lesion in all 9 (100%) successfully imaged iris melanomas and 25 of 35 iris nevi (71%) ($P = .09$) (Table 3). Of the 10 cases with no visible lesion vessels, 8 cases (80%) did demonstrate vessels outside the lesion, indicating that the OCTA technique was feasible, but lesion characteristics (such as significant masking, or absence of vessels) caused a reduced vascular signal.

In healthy iris tissue, radially oriented vessels were seen (Figure 4). The vasculature was remarkably more pronounced in the posterior layers of iris stroma than in the anterior layers (Figure 4). This is consistent with findings from FA studies, describing iris veins (which are larger and more tortuous than arteries) located in the posterior stroma.[38]

TABLE 3. Comparing OCTA Features among Various Lesions[f]

	Conjunctival Melanoma	Conjunctival Nevi	PAM		Iris Melanoma	Iris Nevi	
	n = 4	n = 8	n = 6		n = 9	n = 35	
	Cases (%)	Cases (%)	Cases (%)	*P* Value	Cases (%)	Cases (%)	*P* Value
Vessels in lesion							
Present	4 (100)	8 (100)	6 (100)	NA	9 (100)	25 (71)	.09 [a]
Absent	0	0	0		0 (0)	10 (29)	
Vessel visibility							
1 (clear)	1 (25)	2 (25)	1 (17)	1.00 [b]	2 (22)	7 (20)	.071 [b]
2 (medium)	2 (50)	4 (50)	4 (67)		2 (22)	6 (17)	
3 (nonclear)	1 (25)	2 (25)	1 (17)		5 (56)	12 (34)	
Vessels absent					0 (0)	10 (29)	
VD (overall)	n = 4	n = 5	n = 6		n = 4	n = 13	
Median	35.5	32.5	39.4	.14 [c]	31.8	30.5	.82 [d]
VD (selection [e])	n = 3	n = 3	n = 5		n = 4	n = 12	
Median	38.3	37.0	40.3	.26 [c]	31.8	29.8	1.00 [d]

NA = not applicable; PAM = primary acquired melanosis; VD = vessel density.
[a]Fisher Exact test.
[b]Linear-by-linear test.
[c]Kruskal-Wallis test.
[d]Mann-Whitney *U* test.
[e]The selection of lesions with a light/medium pigmentation and grades 1-2 image quality.
[f]Reported are patients whose imaging scans were "acceptable." *P* values refer to the comparison of all conjunctival lesions, and all iris lesions, respectively.

Tortuous patterns were visible in iris melanoma as well as nevi (Figure 5). Image quality was graded as good or medium in 4 cases (44%) of melanoma and 13 cases (37%) of nevi. Image quality was better in amelanotic or lightly pigmented lesions than in those with dark pigmentation and in those who were younger age than those who were older (Figure 5, Table 2). In cases with ectropion uveae, it was seen that the OCTA signal was blocked, causing a shadow on the cross-sectional B-scan, and an apparent avascular area on the en-face OCTA (Figure 5). We did not see clear differences in vascular patterns between iris nevi and melanoma. The signal tended to be more often absent or of low quality in nevi; however, that could have been due either to masking or because of a truly reduced vascular density ($P = .07$).

The median VD of light or medium pigmented iris melanoma was 31.8% (n = 4); for iris nevi this was 29.8% (n = 12) ($P = .99$). The median VD of all iris lesions combined was 30.5%, this was significantly less than the median VD of paired healthy iris tissue of contralateral eyes (n = 15) (35.6%, $P = .012$).

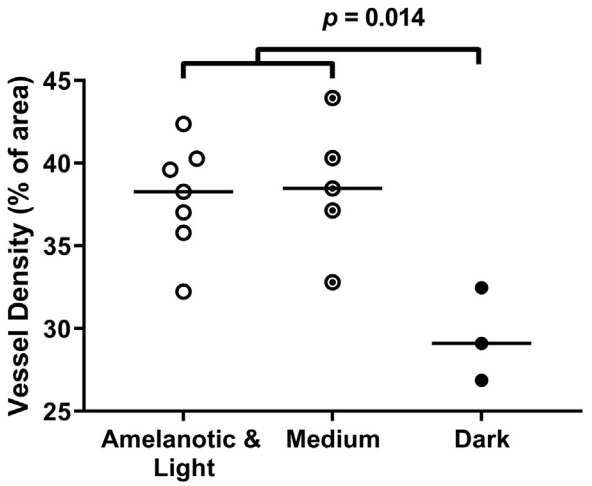

FIGURE 3. Vascular density and pigmentation of conjunctival lesions. The VD was higher in lightly pigmented lesions compared to dark lesions ($P = 0.014$), suggesting a masking effect due to pigment. VD = vessel density.

DISCUSSION

VARIOUS MELANOCYTIC LESIONS OF THE ANTERIOR segment were studied using OCTA. To the authors' knowledge, this is the first report of OCTA in melanocytic lesions of the conjunctiva, and the largest study of OCTA in melanocytic lesions of the iris. Vessels were depicted in all conjunctival and most iris lesions. Obtaining good quality images depended largely on patient cooperation, lesion location, and tumor pigmentation. Significantly better

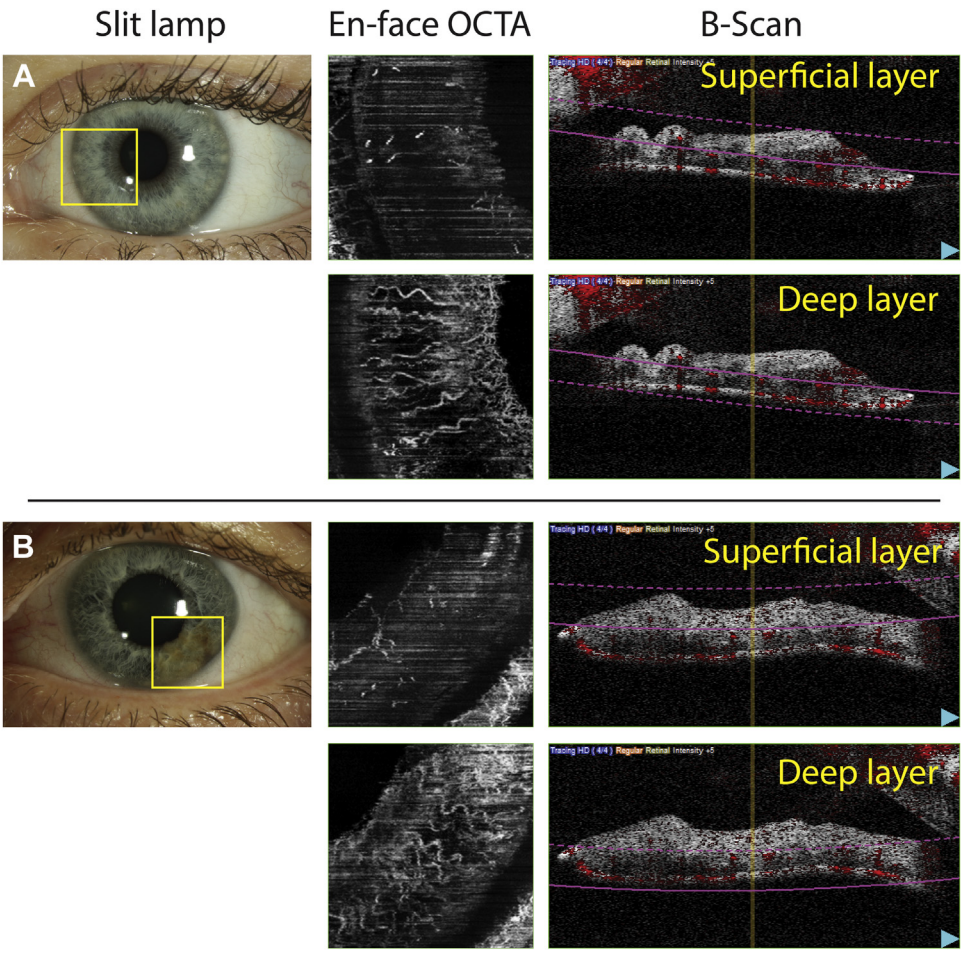

FIGURE 4. Iris vessels at different depths of tissue. (A) In a healthy iris, the radial pattern of iris vessels was clearly visible with OCTA. The vasculature was often more pronounced in the deep (posterior) layers of the iris than in the superficial (anterior) layers. (B) The vessels (iris nevus) may be intrinsic to the tumor or derived from normal vessels. All OCTA scans were acquired in a 3 × 3-mm setting. OCTA = optical coherence tomography angiography.

imaging was seen in lightly pigmented lesions and younger patients. Although vascular patterns of the melanocytic lesions were distinct from healthy tissue, no differentiating OCTA features were found between nevi and melanoma of either the conjunctiva or iris.

Tortuous vascular patterns were detected in both conjunctival nevi and melanoma, which was different from PAM, which apparently lacked an intrinsic vasculature. No vascular patterns or VD measurements were observed that discriminated between conjunctival nevi and melanoma, apart from avascular areas in nevi due to cysts. The absence of distinct vessels in PAM might have been due to confinement to epithelium, not requiring internal vessels as with thicker nodular lesions; the apparent finer meshwork compared to normal conjunctiva may be due to masking by pigment.

Few studies of OCTA of the conjunctiva exist. Healthy conjunctiva has been studied using OCTA resulting in a better visibility of vessels compared to biomicroscopy.[25,35] In a single conjunctival hemangioma, OCTA depicted vasculature better than conventional FA.[39] Recently, OCTA of the conjunctiva and cornea was reported to be better at detecting ischemia compared to clinical examination in patients with chemical injury,[40] and OCTA proved feasible in pinguecula and pterygia,[41] and ocular surface squamous neoplasia.[42]

Some authors have studied vasculature in conjunctival melanoma using immunohistochemistry. Tuomaala and associates[43] quantified vessels in 56 samples by using endothelial marker CD34 and noted no relationship with tumor thickness or survival. Subjectively, in that work, the micro microvascular density was comparable to uveal melanoma. A later report found less CD34 expression in conjunctival melanoma than in surrounding noncancerous stroma, suggesting it to be a hypovascular tumor, despite VEGF production.[44] Heindl and associates[45] studied lymphatic vessels using immunohistochemistry in 109 samples and found a relationship between the presence of vessels and larger lesions and a worse recurrence and survival

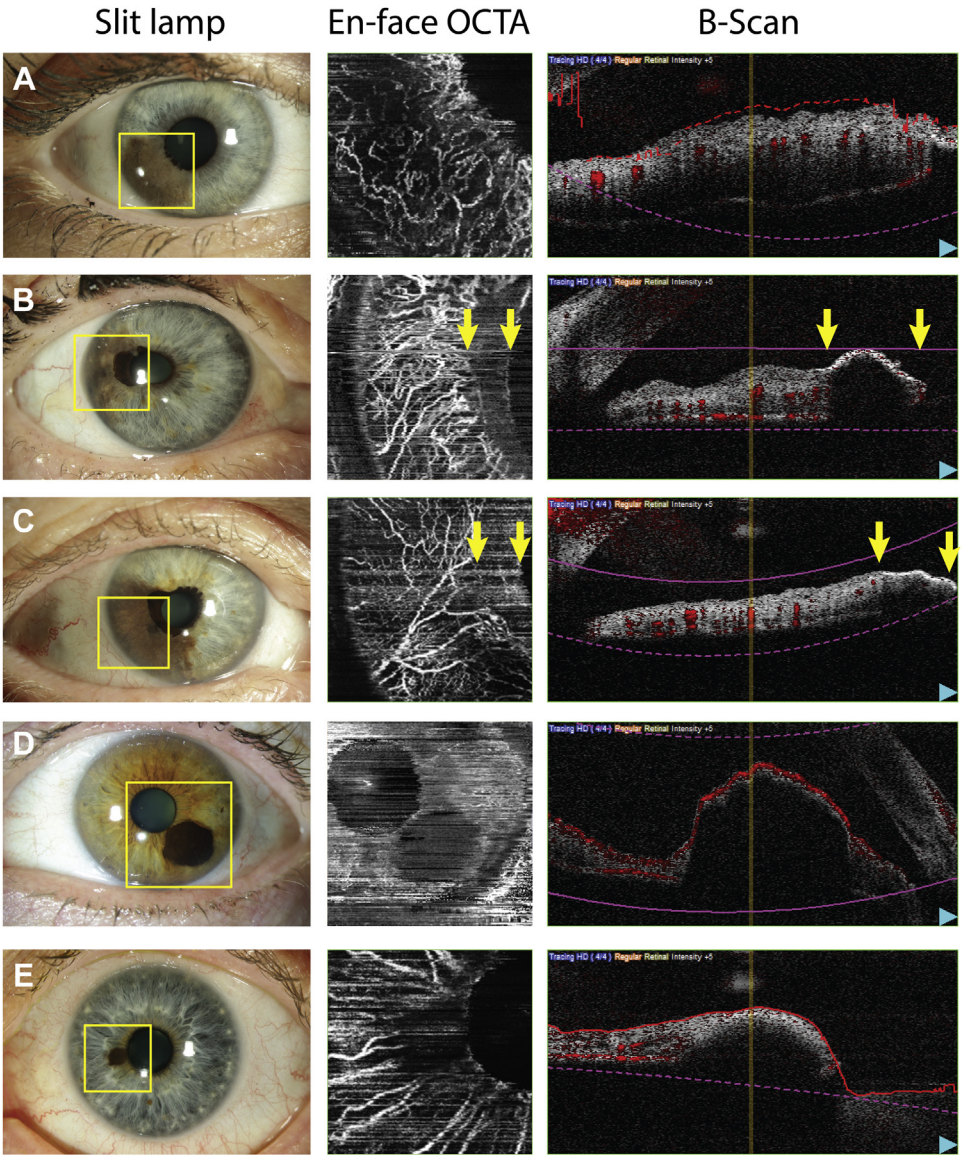

FIGURE 5. Iris melanoma and nevi. Three examples of iris lesions with visible tortuous vascular patterns are shown. (A) Mmelanoma. (B) Melanoma; and (C) nevus. The dark pigmented lesion of Patients D (nevus) and E (nevus) blocked the OCT signal, resulting in an apparent avascular area on OCTA. Similarly, in Patients B and C, the blocking effect of an ectropion uveae was seen. Scans A,B,C, and E were acquired in a 3 × 3-mm setting; scan D was acquired in a 6 × 6-mm setting.

rate. In the present study, however, the authors could not differentiate between blood vessels and lymphatic vessels.

OCTA was used to detect vessels in healthy iris tissue of all but 2 cases. Interestingly, those 2 irises were brown or green, unlike most of the patients, who had blue irises. This was consistent with earlier studies that found that darker iris pigmentation related to worse detection of vessels using OCTA.[46] Iris lesions displayed tortuous patterns, which were clearly distinct from healthy radial vessels (Figures 4 and 5). Different patterns between iris nevi and melanoma were not observed, but vessels tended to be absenct more frequently in iris nevi. This is consistent with earlier reports of FA in iris tumors. Masking has been related to benign lesions, whereas melanoma demonstrated more chaotic patterns.[9–12] The value of these patterns is debated, as geometric patterns were observed in benign lesions as well, and pigment is a known masking factor when using FA.[10,12,13]

The VD in this study did not differ between lightly pigmented iris melanoma (n = 4) and nevi (n = 12). This may not be surprising, considering the small sample size but is remarkably different from earlier observations that described a higher VD in 3 iris melanomas compared to 3 iris nevi.[28] In that work, the presence of darkly pigmented, or cyst-contaning lesions was not reported, however, while that may have influenced measurements.

Alternatively, the present technique might have been less sensitive to changes.

The OCTA device applied in this study (Nidek) uses a spectral domain (SD) technique with an 880-nm wavelength. Present commercially available OCTA devices usually apply either an SD or swept source (SS) technique, with some differences in the underlying technique. SS systems use light of a higher wavelength, allowing visualization of deeper layers, but at a lower resolution.[27] Skalet and associates[28] reported that pigmented lesions of the iris were better imaged with a 1,050-nm technique than with 840 nm, mainly due to tissue penetrance. The present study, in line with others,[35,39] demonstrated that images can be acquired using the SD technique as well but that tissue penetrance is an important limitation, possibly favoring techniques with longer wavelengths.

Our data set was large considering the rarity of the studied diseases but small for statistical analysis. Motion artifacts influenced imaging significantly, resulting in some uninterpretable images and possible underestimation of effects. Motion caused increased "flow," whereas masking or nonpenetrance of the OCT signal caused decreased "flow" (which may explain the decreased VD in iris lesions compared to healthy tissue). The authors, therefore, call for the development of new software to help in image acquisition and analysis (eg, for stabilizing images as in assessment of the retina).

We regard it as a strength that almost all conjunctival lesions in this project were diagnosed by histology. In 3 cases of conjunctival nevus and 1 case of PAM, no tissue was obtained as the clinical diagnosis was clear and not suspicious for malignancy. This is common in clinical management of conjunctival lesions,[2,29,47] and these authors do not believe that obtaining tissue would have influenced results. Even so, a limitation of this study was that iris lesions were usually diagnosed by clinical investigation and ultrasonography only.[30–32] Although there is debate about the exact clinical features of benign and malignant iris lesions,[48] it is common to treat malignant lesions without obtaining histology, and to manage unsuspicious iris lesions by observation.[30,31,33]

Our study showed that OCTA can be used in anterior segment ocular oncology, but better software and enhanced imaging techniques are needed before conclusions about its clinical utility can be drawn. Imaging techniques that are not dependent on light (such as ultrasound biomicroscopy, using sound waves) may be more suitable to depict tumor size,[49] but AS-OCT,[50] and AS-OCTA may provide an additional parameter for differentiating disease (eg, providing reassurance when no abnormal vessels are seen). With better techniques, a prognostic value of angiography may be established. For now, these authors propose that OCTA is most suitable for superficial and nonpigmented disease (eg, lymphoma, ocular surface squamous neoplasia, or basal cell carcinoma) or lightly pigmented melanoma or nevi. As OCTA requires no intravenous dye, with its potential adverse events,[17,18] the use of OCTA may become more widespread than fluorescein angiography or indocyanine green angiography has been up to now.

We conclude that it is feasible to obtain OCTA images of melanocytic lesions of the anterior segment. Good image quality, however, depends highly on patient cooperation and lesion characteristics such as location and pigmentation. New software is called for to improve image acquisition and analysis, and to further develop OCTA analysis of anterior segment lesions. While promising by the noninvasive nature and clinical ease, the role of OCTA in clinical and investigational anterior segment ocular oncology is yet to be established.

ALL AUTHORS HAVE COMPLETED AND SUBMITTED THE ICMJE FORM FOR DISCLOSURE OF POTENTIAL CONFLICTS OF INTEREST and none were reported. This study was supported by the European Commission Horizon 2020 program UM Cure (667787). The sponsors had no role in the design or conduct of this study. N.B. received an MD/PhD programme grant from Leiden University Medical Center, Leiden, The Netherlands. All other authors have reported that they have no relationships relevant to the contents of this paper to disclose.

The authors thank Laméris Ootech BV, Ede, The Netherlands, for providing the imaging device used in this study.

REFERENCES

1. Shields CL, Kaliki S, Hutchinson A, et al. Iris nevus growth into melanoma: analysis of 1611 consecutive eyes: the ABCDEF guide. *Ophthalmology* 2013;120(4):766–772.
2. Shields CL, Shields JA. Tumors of the conjunctiva and cornea. *Indian J Ophthalmol* 2019;67(12):1930–1948.
3. Wong JR, Nanji AA, Galor A, Karp CL. Management of conjunctival malignant melanoma: a review and update. *Expert Rev Ophthalmol* 2014;9(3):185–204.
4. Popovic M, Ahmed IIK, DiGiovanni J, Shields CL. Radiotherapeutic and surgical management of iris melanoma: a review. *Surv Ophthalmol* 2017;62(3):302–311.
5. Bakri SJ, Sculley L, Singh AD. Diagnostic techniques. In: Singh AD, Damato BE, Pe'er J, Murphree AL, Perry JD, eds. Clinical Ophthalmic Oncology. Edinburgh, UK: WB Saunders; 2007:175–180.
6. Oosterhuis JA, van Waveren CW. Fluorescein photography in malignant melanoma. *Ophthalmologica* 1968;156(2):101–116.
7. Cheng H, Bron AJ, Easty D. A study of iris masses by fluorescein angiography. *Trans Ophthalmol Soc U K* 1971;91:199–205.
8. Greite JH. [Fluorescence angiography in iris tumors]. *Ber Zusammenkunft Dtsch Ophthalmol Ges* 1974;72:343–347.

9. Kottow M. Fluorescein angiographic behaviour of iris masses. *Ophthalmologica* 1977;174(4):217–223.
10. Brovkina AF, Chichua AG. Value of fluorescein iridography in diagnosis of tumours of the iridociliary zone. *Br J Ophthalmol* 1979;63(3):157–160.
11. Jakobiec FA, Depot MJ, Henkind P, Spencer WH. Fluorescein angiographic patterns of iris melanocytic tumors. *Arch Ophthalmol* 1982;100(8):1288–1299.
12. Dart JK, Marsh RJ, Garner A, Cooling RJ. Fluorescein angiography of anterior uveal melanocytic tumours. *Br J Ophthalmol* 1988;72(5):326–337.
13. Demeler U. [Control of the course of iris tumors with the aid of fluorescence angiography]. *Adv Ophthalmol* 1978;35:167–178.
14. Christiansen JM, Wetzig PC, Thatcher DB, Green WR. Diagnosis and management of anterior uveal tumors. *Ophthalmic Surg* 1979;10(1):81–88.
15. Bandello F, Brancato R, Lattanzio R, et al. Biomicroscopy and fluorescein angiography of pigmented iris tumors. A retrospective study on 44 cases. *Int Ophthalmol* 1994;18(2):61–70.
16. Meyer PA, Watson PG. Low dose fluorescein angiography of the conjunctiva and episclera. *Br J Ophthalmol* 1987;71(1):2–10.
17. Kwan AS, Barry C, McAllister IL, Constable I. Fluorescein angiography and adverse drug reactions revisited: the Lions Eye experience. *Clin Exp Ophthalmol* 2006;34(1):33–38.
18. Hope-Ross M, Yannuzzi LA, Gragoudas ES, et al. Adverse reactions due to indocyanine green. *Ophthalmology* 1994;101(3):529–533.
19. Spaide RF, Klancnik JM Jr, Cooney MJ. Retinal vascular layers imaged by fluorescein angiography and optical coherence tomography angiography. *JAMA Ophthalmol* 2015;133(1):45–50.
20. Cennamo G, Romano MR, Breve MA, et al. Evaluation of choroidal tumors with optical coherence tomography: enhanced depth imaging and OCT-angiography features. *Eye (Lond)* 2017;31(6):906–915.
21. Toledo JJ, Asencio-Duran M, Garcia-Martinez JR, Lopez-Gaona A. Use of OCT angiography in choroidal melanocytic tumors. *J Ophthalmol* 2017;2017:1573154.
22. Pellegrini M, Corvi F, Invernizzi A, et al. Swept-source optical coherence tomography angiography in choroidal melanoma: an analysis of 22 consecutive cases. *Retina* 2019;39(8):1510–1519.
23. Ang M, Baskaran M, Werkmeister RM, et al. Anterior segment optical coherence tomography. *Prog Retin Eye Res* 2018;66:132–156.
24. Allegrini D, Montesano G, Pece A. Optical coherence tomography angiography in a normal iris. *Ophthalmic Surg Lasers Imaging Retina* 2016;47(12):1138–1139.
25. Akagi T, Uji A, Huang AS, et al. Conjunctival and intrascleral vasculatures assessed using anterior segment optical coherence tomography angiography in normal eyes. *Am J Ophthalmol* 2018;196:1–9.
26. Ang M, Sim DA, Keane PA, et al. Optical coherence tomography angiography for anterior segment vasculature imaging. *Ophthalmology* 2015;122(9):1740–1747.
27. Lee WD, Devarajan K, Chua J, et al. Optical coherence tomography angiography for the anterior segment. *Eye Vis (Lond)* 2019;6:4.
28. Skalet AH, Li Y, Lu CD, et al. Optical coherence tomography angiography characteristics of iris melanocytic tumors. *Ophthalmology* 2017;124(2):197–204.
29. Shields CL, Fasiuddin AF, Mashayekhi A, Shields JA. Conjunctival nevi: clinical features and natural course in 410 consecutive patients. *Arch Ophthalmol* 2004;122(2):167–175.
30. Harbour JW, Augsburger JJ, Eagle RC Jr. Initial management and follow-up of melanocytic iris tumors. *Ophthalmology* 1995;102(12):1987–1993.
31. Conway RM, Chua WC, Qureshi C, Billson FA. Primary iris melanoma: diagnostic features and outcome of conservative surgical treatment. *Br J Ophthalmol* 2001;85(7):848–854.
32. Giuliari GP, Krema H, McGowan HD, Pavlin CJ, Simpson ER. Clinical and ultrasound biomicroscopy features associated with growth in iris melanocytic lesions. *Am J Ophthalmol* 2012;153(6):1043–1049.
33. Oxenreiter MM, Lane AM, Jain P, Kim IK, Gragoudas ES. Conservative management of suspicious melanocytic lesions of the iris. *Graefes Arch Clin Exp Ophthalmol* 2019;257(6):1319–1324.
34. Mehta N, Liu K, Alibhai AY, et al. Impact of binarization thresholding and brightness/contrast adjustment methodology on optical coherence tomography angiography image quantification. *Am J Ophthalmol* 2019;205:54–65.
35. Liu Z, Wang H, Jiang H, Gameiro GR, Wang J. Quantitative analysis of conjunctival microvasculature imaged using optical coherence tomography angiography. *Eye Vis (Lond)* 2019;6:5.
36. Coupland SE, Barnhill RL, Conway M, et al. Conjunctival melanoma. In: Amin MBES, Green F, eds. AJCC Canger Staging Manual. 8th ed. New York: Springer; 2017:795–803.
37. Kivela T, Simpson ER, Grossniklaus HE, et al. Uveal melanoma. In: Amin MBES, Green F, eds. AJCC Cancer Staging Manual. 8th ed. New York: Springer; 2017:805–817.
38. Brancato R, Bandello F, Lattanzio R. Iris fluorescein angiography in clinical practice. *Surv Ophthalmol* 1997;42(1):41–70.
39. Chien JL, Sioufi K, Shields CL. Optical coherence tomography angiography of conjunctival racemose hemangioma. *Ophthalmology* 2017;124(4):449.
40. Fung SSM, Stewart RMK, Dhallu SK, et al. Anterior segment optical coherence tomographic angiography assessment of acute chemical injury. *Am J Ophthalmol* 2019;205:165–174.
41. Zhao F, Cai S, Huang Z, Ding P, Du C. Optical coherence tomography angiography in pinguecula and pterygium. *Cornea* 2020;39(1):99–103.
42. Liu Z, Karp CL, Galor A, et al. Role of optical coherence tomography angiography in the characterization of vascular network patterns of ocular surface squamous neoplasia [Epub ahead of print]. *Ocul Surf* 2020; https://doi.org/10.1016/j.jtos.2020.03.009.
43. Tuomaala S, Toivonen P, Al-Jamal R, Kivela T. Prognostic significance of histopathology of primary conjunctival melanoma in caucasians. *Curr Eye Res* 2007;32(11):939–952.
44. Kase S, Kikuchi I, Ishida S. Expression of VEGF in human conjunctival melanoma analyzed with immunohistochemistry. *Clin Ophthalmol* 2018;12:2363–2367.
45. Heindl LM, Hofmann-Rummelt C, Adler W, et al. Prognostic significance of tumor-associated lymphangiogenesis in malignant melanomas of the conjunctiva. *Ophthalmology* 2011;118(12):2351–2360.
46. Zett C, Stina DMR, Kato RT, Novais EA, Allemann N. Comparison of anterior segment optical coherence tomography

angiography and fluorescein angiography for iris vasculature analysis. *Graefes Arch Clin Exp Ophthalmol* 2018;256(4): 683–691.
47. Gloor P, Alexandrakis G. Clinical characterization of primary acquired melanosis. *Gaz Med Fr* 1995;36(8): 1721–1729.
48. Jakobiec FA, Silbert G. Are most iris "melanomas" really nevi? A clinicopathologic study of 189 lesions. *Arch Ophthalmol* 1981;99(12):2117–2132.
49. Bianciotto C, Shields CL, Guzman JM, et al. Assessment of anterior segment tumors with ultrasound biomicroscopy versus anterior segment optical coherence tomography in 200 cases. *Ophthalmology* 2011;118(7): 1297–1302.
50. Nanji AA, Sayyad FE, Galor A, Dubovy S, Karp CL. High-resolution optical coherence tomography as an adjunctive tool in the diagnosis of corneal and conjunctival pathology. *Ocul Surf* 2015;13:226–235.